phys. stat. sol. (a) **190**, No. 2, 467–475 (2002)

On the Farsightedness (hyperopia) of the Standard k · p Model

Alex Zunger

National Renewable Energy Laboratory, Golden, Colorado 80401, USA

(Received September 4, 2001; accepted September 10, 2001)

Subject classification: 73.20.At; 73.21.Cd; 73.21.La; 73.22.–b; 78.20.Bh

The use of a small number of bands in conventional k · p treatment of nanostructures leads to "farsightedness" (hyperopia), whereby the correct, detailed atomistic symmetry is not seen by the model, but only the global landscape symmetry is noted. Consequently, the real symmetry is confused with a higher symmetry. As a result, a number of important symmetry-mandated physical couplings are unwittingly set to zero in the k · p approach. These are often introduced, after-the-fact, "by hand", via an ansatz. Sometimes physical effects (e.g., piezoelectricity) are invoked to fix the otherwise incorrect symmetry. Thus, whereas in atomistic theories of nanostructures (tight-binding, pseudopotentials) the physically correct symmetry is naturally *forced upon us* by the structure itself, in the standard k · p model it is accommodated *ex post facto* once it is known from sources outside the model itself.

1. Introduction: How Does a Theoretical Model Recognize the Proper Symmetry of the Object Being Modeled? The k · p model [1, 2] was eminently successful [3–6] in modeling the electronic structure of three-dimensional (3D) bulk solids and two-dimensional (2D) quantum wells by expanding their wave functions in just a few, *zone center* (Γ-point) Bloch functions $U_{n,\Gamma}(r)$ of the host crystal:

$$\Psi(r) = \sum_{n}^{N_b} F_n(r)\, U_{n,\Gamma}(r)\,. \tag{1}$$

Using a single band ($N_\mathrm{b} = 1$) gives the "particle-in-a-box" description, whereas use of the valence band maximum alone (six states, $N_\mathrm{b} = 6$, including spatial and spin degeneracies) leads to the "6 × 6 k · p," and addition of the conduction band minimum gives the "8 × 8 k · p." In principle, if one were to use in Eq. (1) a complete basis, this method would be exact (assuming that the interfacial terms are treated correctly [7–9]). However, this is not practical, since in this empirical approach the number of adjustable parameters of the theory increases rapidly with the number of basis functions. Moreover, many of these parameters are not direct physical observables, so they cannot be measured, even in principle. Thus, whereas conventional basis-set expansion methods (e.g., Hartree–Fock for molecules, first-principles plane-wave pseudopotentials for solids) routinely increase their basis sets until convergence is demonstrated, the standard [3–6] k · p model relies instead on a fixed and rather small number of basis orbitals, using adjustable parameters to mitigate variational limitations. This works very well for physical problems where band mixing in Eq. (1) is small, e.g., when studying near-Γ states in bulk solids, wide quantum wells of direct-gap materials, etc. But as the dimensionality is further reduced, and the system becomes more and more different from the reference 3D bulk from which the basis set of Eq. (1) is drawn, additional basis functions may be needed for a reasonable description of the nanostructure wave functions.

0031-8965/02/19004-0467 $ 17.50+.50/0

Table 1

Summary of the atomistic symmetries of a number of nanostructure systems, along with the higher symmetry "seen" by the k · p approach. In the k · p method the lh–hh coupling potentials are zero at the zone center (whereas they are generally non-zero away from the zone center)

System	Correct symmetry	Consequence of symmetry	What does the standard model see?
Film of *N* monolayers	odd or even	*E* vs. thickness oscillates	no reflection symmetry, monotonic *E*
GaAs/AlAs QW or SL	D_{2d}	$V_{\mathrm{lhl,hh2}} \neq 0$, $V_{\mathrm{el,hhl}} \neq 0$ • lhl–hh2 anti-cross • lhl–e2 allowed • hh2–el allowed	$V_{\mathrm{lhl,hh2}} \equiv 0$, $V_{\mathrm{el,hhl}} = 0$ (T_d symmetry)
InAs/GaSb QW or SL	C_{2v}	$V_{\mathrm{lhl,hh1}} \neq 0$ • el–hhl anti-cross • in-plane polariz. anisotropy	$V_{\mathrm{lhl,hh1}} \equiv 0$ • no in-plane polarization (T_d symmetry)
Square based pyramid	C_{2v}	• strain (110) ≠ $(\bar{1}10)$ • p-level splits	C_{4v} symmetry no in-plane polarization; no p-level splitting

This was demonstrated by projecting realistically calculated (i.e., not k · p) wave functions of quantum nanostructures on 3D bulk Bloch function basis [10–15], showing that ~100 Γ bands are often needed for a realistic expansion. One may still hope, however, that even though such a large number of basis functions is needed in principle, in practice one may be able to re-adjust the free parameters of the small basis set theory to match experiment. But one thing is difficult to fix (i.e., is not elegant) by re-parameterization of the existing parameters: the correct symmetry of the object being modeled. If one has just a small number of Bloch functions in Eq. (1), the broad and featureless envelope functions $F_n(r)$ cannot properly resolve the atomistic detail of the object being modeled. Thus, the theory is "hyperopic," noting the global shape but not the detailed symmetry. Table 1 provides a few examples of failing to recognize the correct symmetries. This article explains briefly these cases, and offers a natural alternative.

2. The Oscillating Eigenvalues of a Thin Film A film made of *N* monolayers can be even or odd with respect to the reflection plane at its center. A continuum approach can only tell if the film is, say, 50 Å or 52 Å thick, but not if it has an even or odd number of monolayers. Thus, the odd–even oscillations of the film's eigenvalues, apparent in an *atomistic* calculation [16] (pseudopotential) of Si(001) (Fig. 1), are missed by the "far-sighted" effective-mass approach which gives a monotonic energy vs. film thickness curve.

3. The Oscillating Γ–X Coupling in $(\mathrm{AlAs})_n/(\mathrm{GaAs})_n$ Although small in magnitude ($V_{\Gamma X} \sim 10$ meV), the Γ–X coupling has profound consequences on the properties of the system, leading, for example, to the appearance of indirect transitions without phonon intervention [17, 18], to characteristic pressure-induced changes of the photoluminescence intensity [19, 20], to resonant tunneling in electronic transmission between GaAs quantum wells separated by an AlAs barrier [21], and to level splitting ("avoided crossing") in the pressure-, electric field-, and magnetic field-induced Γ–X transition [22,

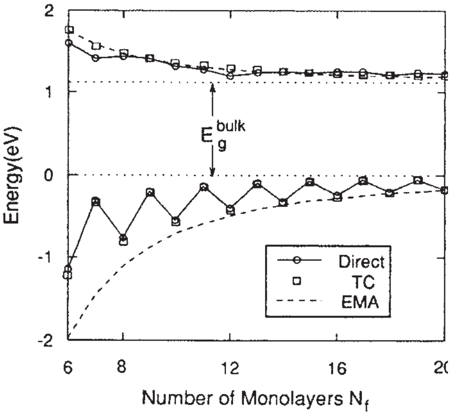

Fig. 1. The size dependence of the highest valence band and lowest conduction band for Si films with N monolayers. The dashed line indicates the effective-mass approximation (EMA) [16]

23]. Atomistic calculations [24] properly recognize the D_{2d} point group symmetry of superlattices having a common atom, such as $(AlAs)_n/(GaAs)_n$. This leads, by symmetry, to a vanishing $V^{(n)}(\Gamma{-}X) = 0$ matrix element for n = odd superlattices, whereas for n = even, a finite coupling is possible, as shown in Fig. 2. In contrast, the conventional $k \cdot p$ model does not "see" the D_{2d} symmetry, confusing it with a higher symmetry. Consequently, the oscillating odd vs. even behavior of the coupling is absent, unless introduced [25] "by hand". This can be done, for example, by adding an artificial external potential at the interface. In contrast, atomistic theories produce naturally the correct oscillations [24] without the need for intervention.

4. The lh1–hh2 Coupling at $K_{\|} = 0$ for Common-Atom Superlattices The D_{2d} symmetry of common-atom superlattices such as InAs/GaAs or AlAs/GaAs permits a non-zero coupling of lh1 and hh2 even at $K_{\|} = 0$ [26–28]. As a result, the lh1 and hh2 bands anti-cross as a function of superlattice period n (Fig. 3) [29]. An additional consequence is that the lh1-to-e2 transition becomes allowed, as is the hh2-to-e1 transition. Conventional $k \cdot p$ does not see the D_{2d} symmetry, confusing it instead with the T_d symmetry of the zinc blende constituents. Consequently, the lh1 *crosses* the hh2 level, and the above-noted transitions are forbidden, unless a correction is introduced by hand [26, 27]. Such corrections involve adding, for example, a fictitious external potential. In contrast, atomistic theories produce naturally the correct behavior [29].

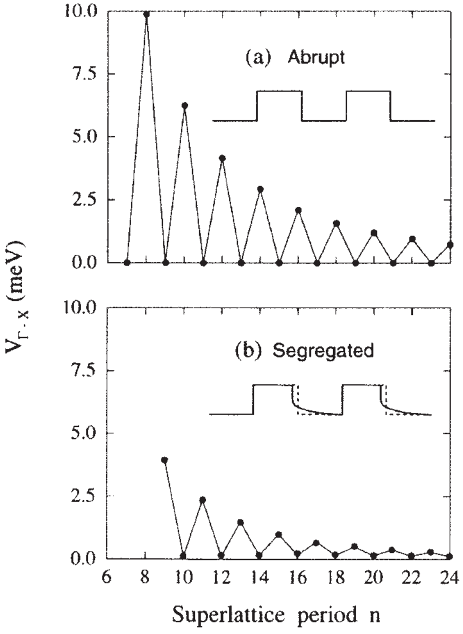

Fig. 2. The Γ–X coupling in AlAs/GaAs superlattices [24]: a) abrupt; b) segregated

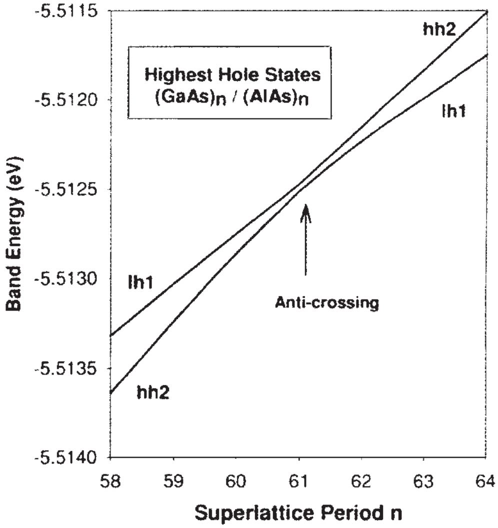

Fig. 3. lh1 and hh2 energy levels in the region of anti-crossing in $(GaAs)_n/(AlAs)_n$ (001) superlattices [29]

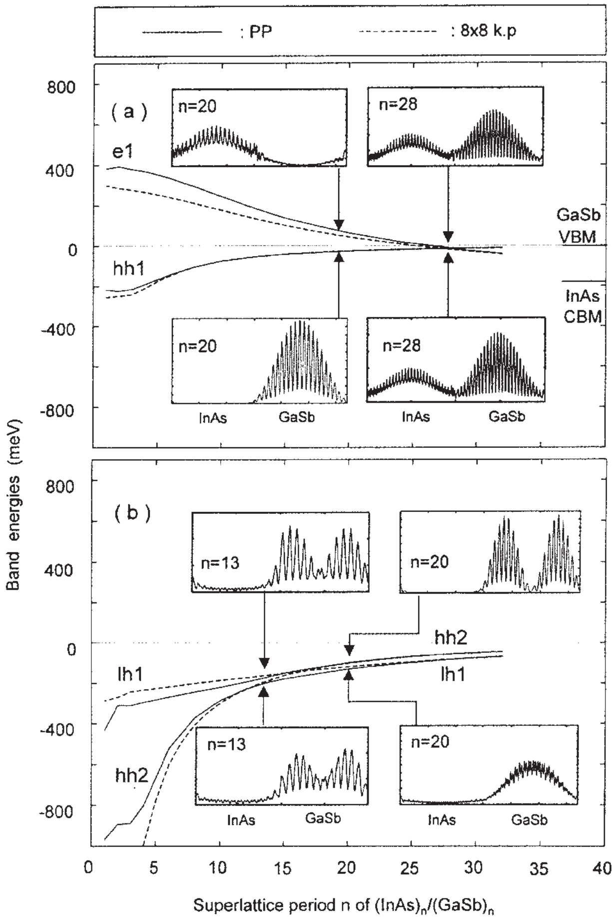

Fig. 4. Anti-crossing in $(InAs)_n/(GaSb)_n$ superlattices [31]:
a) l1–hh1; b) lh1–hh2

5. The lh1–hh1 Coupling at $K_{\|} = 0$ for No-Common-Atom Superlattices In no-common-atom superlattices such as InAs/GaSb or GaAs/InP the symmetry is reduced to C_{2v}, so even lh1 can couple to hh1 [27, 30, 31] at $K_{\|} = 0$. Consequently, lh1 can anti-cross hh1 (Fig. 4) and an in-plane polarization anisotropy $I_{110} \neq I_{\bar{1}10}$ is evident in the lowest transition. Conventional k · p has a vanishing lh1–hh1 coupling at $K_{\|} = 0$, hence no polarization anisotropy. This, however, can be introduced *ex post facto* by hand [26, 27].

6. Quantum Dots and Piezoelectric Charges Another interesting case of failure to recognize symmetry in standard k · p treatment concerns pyramidal quantum dots. If one uses as a model a square-based pyramid, then the macroscopic symmetry is C_{4v}. In this case, continuum-like theories indicate that p-levels are not split and there is no polarization anisotropy for the lowest e–h transition. However, if the square-based pyramid is made of a zinc blende solid such as InAs, the (110)direction is not equivalent to the $(\bar{1}10)$ direction. This reduces the symmetry to C_{2v} [32]. In this symmetry: (a) an in-plane polarization anisotropy emerges [32–34], i.e., the dipole element for the lowest transition along (110) differs from that along $(\bar{1}10)$, the polarization ratio thus being $\lambda \neq 1$; (b) the otherwise doubly degenerate p levels split; and (c) the s-like electron wave function is rotated (in "anti-phase") with the s-like hole wave function. The real, C_{2v} symmetry of an atomistic square-based pyramid exists already even if the dot is unstrained, i.e., an "uncapped" freestanding InAs dot will already have this symmetry. If a capping barrier material strains the dot (e.g., GaAs on InAs dots) the atomic relaxation follows the atomic symmetry. Thus, the strain will also have C_{2v} symmetry. (However, describing strain via continuum elasticity incorrectly gives C_{4v} symmetry [33].) Thus, the polarization anisotropy, the p-level splitting, and wave function anti-phase all emerge from (a) the atomically imposed C_{2v} symmetry of the unstrained zinc-blende system, and (b) the atomistic strain. Effect (a) is much larger than effect (b), as the latter produces only weak polarization anisotropy.

Conventional k · p treatment misses the C_{2v} symmetry of a square-based zinc blende pyramid, and along with it the in-plane anisotropy, the p-level splitting, and the wave function anti-phase [35]. One can, however, cause p-level splitting by introducing the piezoelectric effect [36]. In zinc blende dots such piezoelectric charges exist only near the sharp edges of the *faceted* quantum dot, e.g., an ideal *pyramidal* dot, but rounded objects have nearly vanishing piezoelectric charges. Indeed, many of the k · p calculations have insisted on an ideal, faceted *pyramidal shape*, since only for such shapes is there a significant piezoelectric effect. In the k · p approximation the piezoelectric effect is *required* in order to create p-level splitting, polarization anisotropy, and wave function anti-phases, all of which are observed effects. These effects all disappear in k · p treatment in the absence of a piezoelectric field. In an atomistic description, such as pseudopotential, all of these effects emerge naturally *without* assuming piezoelectric fields, simply because the atomic description yields naturally the C_{2v} symmetry. Thus, introduction of the piezoelectric field is a device, used in k · p models, to mimic the correct, but otherwise neglected atomistic symmetry of the dot. One can always add the piezoelectric effect to the pseudopotential calculations. (Note that in order to compare "apples with apples," one must compare k · p *without* piezoelectric field to pseudopotential results also *without* piezoelectric field. This was done in Ref. [35]. It is incorrect to compare k · p *with* this effect to pseudopotential *without* this effect, as was done in Ref. [36].)

The question then is how big are piezoelectric fields in commonly grown dots? This question is equivalent to asking whether currently grown dots have sharp and well-defined edges and facets, once they are capped. The author's impression is that most capped dots are rather round without sharp edges, exhibiting instead segregation and intermixing [37, 38]. Such objects (e.g., lens-shaped dots) have negligible piezoelectric charges. Nevertheless, in an atomistic description such dots have C_{2v} symmetry. Although calculations for faceted ideal pyramidal dots are convenient for comparing computational schemes, they do not have much physical reality for InAs/GaAs, whereas rounded, interdiffused lens-shaped dots are more realistic. Such dots have virtually no piezoelectric fields. But then k · p will predict no p-level splitting, no polarization anisotropy, and no wave function anti-phase, in conflict with experiment. Pseudopotential calculations exhibit these effects even for lens-shaped dots.

7. Keep Fitting until Agreeing with Atomistic Theory or Experiment on Dots? Another approach taken by k · p models is to change material constants (e.g., effective masses) until agreement with a desired set of data is achieved while fitting parameters to reproduce the properties of the underlying *bulk* solid seems reasonable, re-adjusting these parameters to fit the measured properties of the *nanostructure* itself appears questionable. For example, consider k · p calculations on CdSe dots. Norris and Bawendi [39] say: "We use standard nonlinear least-squares method to globally fit the experimental data ... our fitting routine adjusts three parameters: the Luttinger band parameters γ_1 and γ_2 ... and the potential barrier for electrons." According to Efros et al. [40], "The position of the quantum size levels are very sensitive to the valence band energy parameter; those used for calculation give the best description of the CdSe microcrystal absorption spectra." Wind et al. [41] say: "Fig. 1 shows the experimental values the lines in Fig. 1 have been calculated following a model including the valence mixing The best correspondence could be obtained [by] choosing a Luttinger parameter $\gamma = 0.38$..." Since in these cases the k · p theory is explicitly fit to experiment on dots, it cannot examine the legitimacy of either its successes or its failures.

Another version of fitting is provided by the work of Stier et al. [42] responding to earlier pseudopotential work of Wang et al. [35]. To assess the validity of the 8-band k · p model, Wang et al. performed a simple test, contrasting k · p with a full atomistic pseudopotential calculation, using a *common microscopic input*. Specifically, they used the atomic pseudopotentials of InAs and GaAs, obtaining the standard bulk band structures. From these bulk band structures they calculated the bulk electron and hole effective mass tensors at the zone center. Using these effective masses (that were in excellent agreement with bulk measurements) they computed the k · p Luttinger parameters from standard equations. These Luttinger parameters were then used in an 8-band k · p program to compute the energy levels of the pyramidal InAs/GaAs dot, neglecting piezoelectric effects. Analogous results (which we call "standard k · p") are shown in Fig. 2e of Stier et al. [42]. Independently, the same atomic pseudopotentials were used by Wang et al. [35] to compute directly (without k · p) the energy levels of the same pyramidal dot, also neglecting piezoelectric effects. Analogous results ("pseudopotential") are shown in Fig. 2b of Stier et al. [42]. By comparing the two sets of results (k · p and pseudopotential) one could assess the validity of using 8 bands vs. using a converged number of bands, all other things being the same. The results of Wang et al. clearly demonstrated some shortcomings of k · p, the most significant being (i) a reduced splitting of the electron p states (3 vs. 24 meV), (ii) an incorrect in-plane polarization ratio for electron–hole dipole transitions (0.97 vs. 1.24), and (iii) an over confinement of both electron (by 48 meV) and hole (by 52 meV) states, resulting in a band gap error of 100 meV.

Similar tests for the k · p treatment were done for freestanding dots of InP passivated with hydrogen [14]. The diameter of these dots, 30 Å–50 Å, is actually not small; it is typical of the confining dimension (i.e., height) of most self-assembled dots. Again, doing side-by-side k · p and pseudopotential calculations based on the same input bulk band structure reveals important differences [14] including: (i) incorrect k · p symmetry for the first hole state (p envelope instead of s envelope, leading to the prediction that the ground state P_h–S_e exciton is forbidden); (ii) about 60% of the hole energy levels in the first 500 meV below the VBM are missing in k · p, on account of an exaggerated confinement; (iii) the second to fifth electron states that in a pseudopotential calculation are made of bulk L_{1c} bands are missing altogether in k · p; and (iv) the "intrinsic gap states" found [43] in k · p for pure, defect-free InP dots were shown [44] to originate from a mathematical instability in the equations, thus, not being a physical effect. Such gap states are absent in a direct pseudopotential calculation. Clearly, because of (i)–(iv) above, the interpretation of the spectra of InP dots via k · p was rather unusual, involving spatially forbidden ground state excitons, sparsely spaced hole states, and transitions to/from intrinsic gap states. None of these conclusions is supported by experiment.

Stier et al. [42] proposed another fix to the k · p shortcomings: they altered the bulk effective masses (thus, the Luttinger parameters) to better fit the pseudopotential results. This is illustrated in their Fig. 2d (which we call "k · p with modified masses"). The new bulk effective masses are not reported. Although this modification brings the k · p closer to the pseudopotential results (compare their Fig. 2d with 2b), the agreement is not satisfactory, since the polarization ratio is still close to unity, the p levels (C1, C2) are virtually unsplit, and the wave functions (not shown in Ref. [42]) are still oriented incorrectly. Furthermore, the hole states are ~50 meV too deep, as are the electron states. As a further fix, Stier et al. added the piezoelectric correction to the modified k · p results (Fig. 2c). They then compared these results containing the piezoelectric correction (Fig. 2c) with the direct pseudopotential result that lacked the piezoelectric correction (Fig. 2b), finding now good agreement for energies as well as wave functions. Unfortunately, they neglected to add the piezoelectric correction to the pseudopotential result, a correction that for a pyramidal dot must significantly enhance the polarization ratio, p-level splitting, and wave function orientation. In my view, this comparison is not meaningful, as is the use of the effective masses as adjustable parameters.

8. The Main Point

We see that the k · p approach with a small basis cannot resolve atomistic detail, thus missing in its farsightedness the correct symmetry, "seeing the nanostructure through a frosty glass". This means that symmetry-related physical effects such as level anti-crossing, degeneracy removal, polarization anisotropy, and some state mixing are ignored. All of these effects exist naturally in a theory that uses a basis set with sufficient resolution, i.e., using an atomistic approach. The current culture of k · p practitioners appears to be different: rather than improve the resolution of their "microscope," they prefer to keep a low-resolution (small basis set) approach and impose the correct symmetry by adding external parameters (new potential terms in the Hamiltonian). Such potentials take the form of piezoelectric charges in dots or interfacial charges in superlattices. The degree to which such external potentials are really physical remains questionable. Furthermore, the values of such potential matrix elements are not provided by the k · p model itself, but must be provided externally (unless one uses a complete theory; see Refs. [7–9]). Thus, whereas in atomistic theories of nanostructures [10–16, 24, 30, 35] the correct physical symmetry is forced upon us by the structure itself, the standard k · p model can only accommodate it once it is known from other sources. It seems that 45 years after the invention of the k · p approach [1], the time has come to treat nanostructures by more refined approaches, where the Hamiltonian contains atomistic physics and the basis set has sufficient resolution to see it. It turns out that such approaches (e.g., see the short reviews in Ref. [45]) are both accurate and easy to use. They have also been recently programmed independently by others [46, 47].

References

[1] J.M. LUTTINGER and W. KOHN, Phys. Rev. **97**, 869 (1955).
[2] E.O. KANE, J. Phys. Chem. Solids **1**, 249 (1957).
[3] M. CARDONA and F.H. POLLAK, Phys. Rev. **142**, 530 (1966).
[4] G. BASTARD, J.A. BRUM, and R. FERREIRA, in: Solid State Physics, Vol. **44**, Ed. D. TURNBULL and H. EHRENREICH, Academic Press, New York 1991 (p. 229).
[5] G. BASTARD, Wave Mechanics Applied to Semiconductor Heterostructures, Les Editions de Physique, Paris 1990.
[6] G.A. BARAFF and D. GERSHONI, Phys. Rev. B **43**, 4011 (1991).
[7] M.G. BURT, J. Phys.: Condens. Matter **4**, 6651 (1992).
[8] M.G. BURT, Phys. Rev. B **50**, 7518 (1994);
Appl. Phys. Lett. **65**, 717 (1994).
[9] B.A. FOREMAN, Phys. Rev. Lett. **81**, 425 (1998).
[10] D.M. WOOD and A. ZUNGER, Phys. Rev. B **53**, 7949 (1996).
D.M. WOOD, A. ZUNGER, and D. GERSHONI, Europhys. Lett. **33**, 383 (1996).
[11] A. FRANCESCHETTI, S.H. WEI, and A. ZUNGER, Phys. Rev. B **52**, 13992 (1995).
[12] A. FRANCESCHETTI, S.H. WEI, and A. ZUNGER, Phys. Rev. B **50**, 8094 (1995).
[13] L.W. WANG and A. ZUNGER, Phys. Rev. B **54**, 11417 (1996).
[14] H. FU, L.W. WANG, and A. ZUNGER, Appl. Phys. Lett. **71**, 3433 (1997);
Appl. Phys. Lett. **73**, 115 (1998).
H. FU and A. ZUNGER, Phys. Rev. B **57**, R15064 (1998).
[15] H. FU, L.W. WANG, and A. ZUNGER, Phys. Rev. B **57**, 9971 (1998).
[16] S.B. ZHANG and A. ZUNGER, Appl. Phys. Lett. **63**, 1399 (1993).
S.B. ZHANG, C.Y. YEH, and A. ZUNGER, Phys. Rev. B **48**, 11204 (1993).
[17] M. NAKAYAMA et al., Solid State Commun. **88**, 43 (1993).
[18] V. VOLIOTIS et al., Phys. Rev. B **49**, 2576 (1994).
[19] M. HOLTZ et al., Phys Rev. B **41**, 3641 (1990).
[20] G.H. LI et al., J. Phys. Chem. Solids **56**, 385 (1995);
Phys. Rev. B **50**, 18420 (1994).
[21] E.L. IVCHENKO et al., Solid-State Electron. **37**, 813 (1994).
[22] M.H. MEYNADIER et al., Phys. Rev. Lett. **60**, 1338 (1988).
[23] N.J. PULSFORD et al., Phys. Rev. Lett. **63**, 2284 (1989).
[24] L.W. WANG and A. ZUNGER, Phys. Rev. B **56**, 12395 (1997);
Phys. Rev. Lett. **78**, 2219 (1997).
[25] G.F. GLIASKII, V.A. LAKISOV, A.G. DOLMATOV, and K.V. KRAVCHENKO, Nanotechnology **11**, 233 (2000).
[26] E.L. IVCHENKO, A.H. KAMINSKI, and U. ROSSLER, Phys. Rev. B **54**, 5852 (1996).
[27] O. KREBS and P. VOISIN, Phys. Rev. Lett. **77**, 1829 (1996).
O. KREBS, D. RONDI, J.L. GENTNER, L. GOLDSTEIN, and P. VOISIN, Phys. Rev. Lett. **80**, 5770 (1998);
Eur. Phys. J. **B21**, 241 (2001).

[28] R.C. Miller, A.C. Gossard, G.D. Sanders, Y.-C. Chang, and J.N. Schulman, Phys. Rev. B **32**, R8452 (1985).

[29] R. Magri and A. Zunger, Phys. Rev. B **62**, 10364 (2000).

[30] R. Magri, L.W. Wang, A. Zunger, I. Vurgaftman, and J.R. Meyer, Phys. Rev. B **61**, 10235 (2000).

[31] L.W. Wang, S.H. Wei, T. Mattila, A. Zunger, I. Vurgaftman, and J.R. Meyer, Phys. Rev. B **60**, 5590 (1999).

[32] J. Kim, L.W. Wang, and A. Zunger, Phys. Rev. B **57**, R9408 (1998).

[33] C. Pryor, J. Kim, L.W. Wang, A. Williamson, and A. Zunger, J. Appl. Phys. **83**, 2548 (1998).

[34] L.W. Wang, J. Kim, and A. Zunger, Phys. Rev. B **59**, 5678 (1999).

[35] L.W. Wang, A.J. Williamson, A. Zunger, H. Jiang, and J. Singh, App. Phys. Lett. **76**, 339 (2000).

[36] O. Stier, Electronic and Optical Properties of Quantum Dots and Wires, Berlin Studies in Solid State Physics, Vol. 7, Wissenschaft & Technik Verlag, Berlin 2001.

[37] I. Kegel et al., Phys. Rev. B **63**, 035318-1 (2001).

[38] J. Shumway et al., Phys. Rev. B **64**, 125302 (2001).

[39] D.J. Norris and M.G. Bawendi, Phys. Rev. B **53**, 16338 (1996).

[40] A. Efros, V.A. Kharchenco, and M. Rosen, Solid State Commun. **93**, 281 (1995).

[41] O. Wind, F. Gindele, and U. Woggon, J. Lumin. **72–74**, 300 (1997).

[42] O. Stier, R. Heitz, A. Schliwa, and D. Bimberg, phys. stat. sol. (a) **190**, 477 (2002) (this volume).

[43] P.C. Sercel, A.L. Efros, and M. Rosen, Phys. Rev. Lett. **83**, 7394 (1999).

[44] L.W. Wang, Phys. Rev. B **61**, 7241 (2000).

[45] A. Zunger, MRS Bull. **23**, 35 (1998);
phys. stat. sol. (b) **224**, 727 (2001).

[46] S. Botti and L.C. Andreani, Phys. Rev. B **63**, 235313 (2001).

[47] F. Chirico, A. DiCarlo, and P. Lugli, Phys. Rev. B **64**, 045314 (2001).